IOSR Journal of Applied Geology and Geophysics (IOSR-JAGG)
e-ISSN: 2321–0990, p-ISSN: 2321–0982.Volume 6, Issue 5 Ver. II (Sep. – Oct. 2018), PP 01-18
www.iosrjournals.org

Seismic Velocity Model for Sedimentary Niger Delta, Nigeria

[1]E. D. Uko, [2]J. O. Ebeniro, [3]C. O. Ofoegbu and [4]G. I. Alaminiokuma,
[1]*Department of Physics, Rivers State University of Science and Technology, PMB 5080, Port Harcourt, Nigeria*
[2]*Department of Physics, University of Port Harcourt, Port Harcourt, Nigeria.*
[3]*Institute of Geosciences and Earth Resources, Nasarawa State University, Keffi, Nigeria.*
[4]*Department of Physics, Federal University of Petroleum Resources, Effurun, Delta State, Nigeria.*
Corresponding Author: 1E. D. Uko,

Abstract: *A seismic velocity model that better approximates the effects of the gradually increasing velocities with depth due to compaction in clastic sediments is invested in the clastic sediment in Agbada Field in the Niger Delta in Nigeria. The velocity data were computed from seismic refraction survey. The time-distance data obtained were observed to yield to the theory of linear increase of velocity with depth; hence the curves generated were hyperbolic in shape. This formed the basis of computation of the model parameters: V_o (top-interface velocity) and k (vertical velocity gradient) by solving the hyperbolic sine equation [Sinh(kt/2) = (kx/2V_o) analytically. Graphical profiles were plotted using Microsoft Xcel software. The velocity function is represented as: V = 1712.70 + 1.083z. Constructions of raypaths originating from the shot point and emerging at each geophone position were observed to be arcs of circles as obtainable in a case of linear increase of velocity with depth. Similarly constructed wavefronts at the various values of arrival time, T with the equivalent values of k and V_o were observed to be curves which crossed the raypaths at right angles. These results are consistent with theory and go further to show that the developed model obeys all the laws of refraction. The interpreted field data give average values of V_o and k to be 1712.70ms^{-1} and 1.083s^{-1} respectively. This method provides a basis for predicting the lateral and vertical velocity structure of the subsurface clastic sedimentary Niger Delta basin using a relatively small layer thickness with the assumptions that lithologies are sharply discontinuous and discrete are not considered and this will bring into play the recognition of change in facies, fractures, faults, unconformities and so on and this true in actual field situations. The modelled V_o and k values could also be used as estimates in any part in the study area prior to detailed exploration in the region.*

Key words*: Velocity, clastic sediments, hyperbolic time-depth curves, wave fronts, wave paths, Central Depobelt, Niger Delta, Nigeria.*

Date of Submission: 01-10-2018 *Date of acceptance: 16-10-2018*

I. Introduction

Velocity gradually increases with depth because of the effect of compaction. Several velocity models have been suggested to describe the velocity profile in clastic sediments. The simplest one is the piecewise-constant model with a number of horizontal layers of different constant velocities [1, 2]. More complex models assume that velocity varies in a systematic continuous manner. Of considerable importance is the linear increase of velocity with depth that is generally accepted and often confirmed by measurements of thin clastic rocks [3].

The conventional method of computing seismic velocity data has been to fit time-distance plots as discrete linear segments, assuming that velocity is constant within each medium, ray paths are straight, layering is in discrete steps in a sedimentary region with clastic materials and that true increase in velocity continues downward indefinitely. These assumptions may mean no faults, no unconformities, no facies change and no fractures within the subsurface. Conversely, velocity computations by analytic functions especially, the linear distribution of velocity with depth fits time-distance plots as hyperbolic sine curves, assuming that velocity varies in a systematic continuous manner and ray paths are arcs of circles. This later model is a refinement over the use of the former. In actual practice, this type of model is sufficiently good so that it serves as a very excellent approximation of the actual velocity function that is more realistic in many sedimentary basins [4]. One of such sedimentary basins in which this type of model has been applied is the United States coast of Gulf of Mexico which shows much similarity to the Niger Delta. Uko *et al*. [5] obtained a velocity gradient of 8.5s^{-1} for east central Niger Delta in Nigeria.

Modelling the subsurface velocity structure of the Niger Delta Basin applying the linear distribution of velocity with depth function is the major concern of this present work and is aimed at avoiding some of the limitations introduced by the assumptions due to the piecewise-constant velocity model mentioned above. Its objectives are to derive a robust computational model that closely predicts lateral and vertical velocity structure

of the Niger Delta, to derive a velocity gradient that can be used to determine the velocity at the depth of the weathered layer in the absence of any other information prior to exploration in the region, and to provide a characteristics reference model for the several areas of research that depend on the subsurface velocity structure of the Niger Delta in their analyses. Moreover, a velocity model of the subsurface-clastic sediments of the Niger Delta can be useful in detection of structures at varying depths, migration and lithologic investigations, stratigraphic detailing at different intervals of depth, conversion of time to depth section, and in detection of overpressured zones.

II. Geology of the Study Area

The Niger Delta occurs at the Southern end of Nigeria bordering the Atlantic Ocean and located between Longitude 4º - 9º E and Latitudes 4º - 6º N with the sub-aerial portion covering about 75,000km² extending more than 300km from apex to mouth (Fig. 1). The regressive wedge of clastic sediments which it comprises is thought to reach a maximum thickness of about 12km [6].

As in many deltaic areas, it is extremely difficult to define a satisfactory stratigraphic nomenclature [6]. The interdigitation of a small number of lithofacies makes it impossible to define units and boundaries of sufficient integrity to constitute separate formations in a formal sense. However, three formation names are in wide-spread use [7, 8], corresponding to the portions of the tripartite sequence (Fig. 2) ranging in age from Eocene to Holocene. The primary source rock is the upper Akata Formation, the marine-shale facies of the delta, with possible contribution from interbedded marine shale of the lowermost Agbada Formation. Oil is produced from sandstone facies within the Agbada Formation, however, turbidite sand in the upper Akata Formation (Fig. 2) is a potential target in deep water offshore and possibly beneath currently producing intervals onshore. The Akata Formation with an average thickness of at least 4500 m, consisting of marine clays with silty and sandy interbeds [9].

A variety of structural trapping elements exists, including those associated with simple rollover structures; clay filled channels, structures with multiple growth faults, structures with antithetic faults, and collapsed crest structures. The primary seal rock in the Niger Delta is the interbedded shale within the Agbada Formation. The shale provides three types of seals-clay smears along faults, interbedded sealing units against which reservoir sands are juxtaposed due to faulting, and vertical seals. The Agbada Formation, which is characterized by Paralic to marine-coastal and fluvial-marine deposits mainly composed of sandstones and shale organized into coarsening upward offlap cycles. The Benin Formation consists of continental and fluvial sands, gravel, and backswamp deposits (2500 m thick).

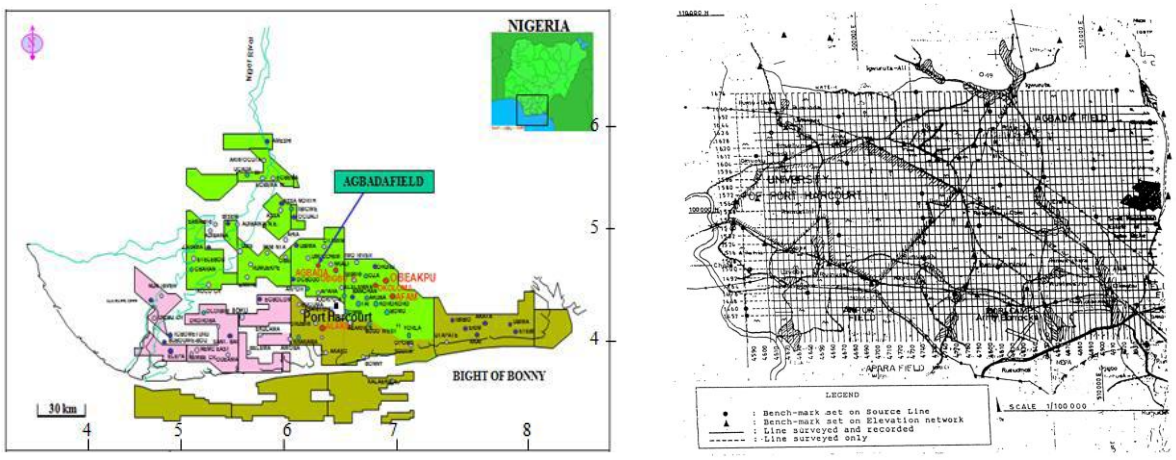

Fig. 1: Map of the Niger Delta showing the Agbada 3-D Program Map with Receiver and Source Lines.

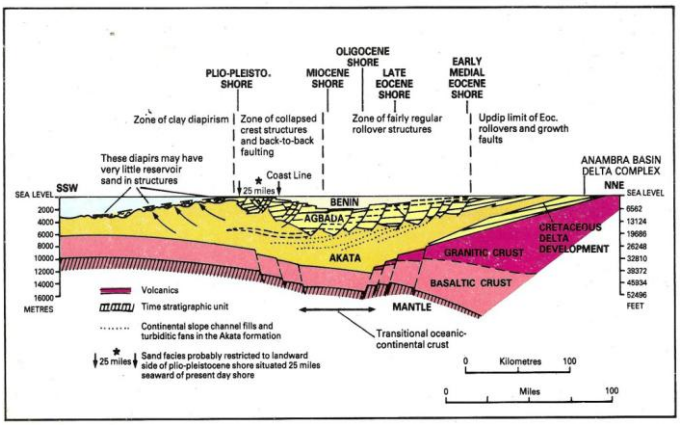

Fig. 2: The Different Lithofacie in the Niger Delta [9].

III. Theoretical Background

3.1 Seismic Velocity Variation

Seismic velocity, the speed of seismic waves in different geologic strata, is a key parameter in seismic processing and interpretation. The knowledge of seismic velocity variation trend at any particular depth and lateral extent is very important in the recognition of reflectors and refractors with dip or horizontal beds. Variations in the thickness and velocity of layers are most pronounced near the surface because of the process of weathering which produces a layer of inhomogeneous and unconsolidated material at the earth's surface called the weathering (low velocity) layer. With older beds at depth, sediment velocities usually show only small variations except where the type of sediments change quickly, such as with reefs, salt domes, and faults.

The assumption of constant velocity is not valid in general, the velocity usually changes as we go from one point to another in the subsurface. The changes in seismic velocity in the horizontal direction in more-or-less flat-lying bedding are for the most part small, being the result of slow changes on density and elastic properties of the beds. These horizontal variations are generally much less rapid than the variations in the vertical direction where we are going from bed to bed with consequent lithological changes and increasing pressure with increasing depth.

3.2 Velocity Functions

The variation of seismic velocity with depth and time is a fundamental aspect of seismic work. Several velocity models have been suggested to describe the velocity profile in sedimentary layers. The simplest one is the piecewise-constant model with a number of horizontal layers of different, constant velocities given by Dix [1] and Hubral [2]. A comprehensive description of linear model can be found in the work by Slotnick [3]. Higher order velocity functions, such as the classical exponential trend, parabolic, or Faust law, have been developed to describe the velocity distribution within thicker layers. The classical instantaneous linear velocity model is:

$$V_o(z) = V_a + kz \qquad (1)$$

and the classical exponential model (Slotnick, 1936) is:

$$V_o(z) = V_A \exp\left(\frac{k_a z}{V_a}\right) \qquad (2)$$

The classical exponential models are limited because they tend towards infinite velocity with increasing layer thickness. Parameter V_a is the top-interface instantaneous velocity, k is a constant vertical gradient in the linear model and k_a is the gradient at the top interface in the exponential model. Moreover, in Slotnick's exponential model the gradient increases with depth which is in contradiction to the expected behaviour. For large thicknesses, these models do not represent the actual, physical-compaction effect that occurs in sediment layers.

A more realistic representation was suggested by Faust [10, 11] with:

$$V_o(z) = A\sqrt[n]{z}, n \approx 6 \qquad (3a)$$

where the gradient of velocity decreases with depth. However, this model yields a vanishing velocity at the surface and is still not bounded at large depth. Vanishing velocity at the surface can be avoided by introducing a reference depth:

$$V_o(z) = A \bullet \sqrt[n]{z + z_{\mathrm{Re}\,f}} \qquad (3b)$$

Equivalently written as:

$$V_o(z) = V_a \bullet \sqrt[n]{1 + nk_a z / V_a} \qquad (3c)$$

where the parameters are the top-interface velocity V_a, the top-interface gradient k_a and the root index n.

The parabolic model [12, 13]:

$$V_o(z) = \sqrt{V_a^2 + 2V_a k_a z} \qquad (4)$$

Also represents the decrease of velocity gradient with depth. Like the Faust law, it is unbounded at large depth and therefore limited. Actually, the parabolic model corresponds to the modified Faust with n = 2. Another alternative is the linear decrease of slowness S [14] with depth:

$$S(z) = S_a - Az \qquad (5)$$

Equivalently it can be written in terms of instantaneous velocity:

$$V_o(z) = V_a^2 / (V_a - k_a z) \qquad (6)$$

However, this model suffers because it requires a maximum-allowed depth $z < z_{max} < V_a/k_a$. In addition, the velocity gradient increases with depth, which does not meet the expected geological trend. The quadratic law provides an additional degree of freedom but leads to a decrease in velocity with depth at a definite depth level $z = k_a/h$, where the velocity reaches maximum value:

$$V_o(z) = V_a + k_a z - hz^2 / 2 \qquad (7)$$

The varieties of instantaneous-velocity functions presented by Kauffman [15] include:

(I) $$V = V_0 (1 + kz)^{\frac{1}{n}} \qquad (8)$$

This function is of sufficient generality to cover a number of cases of practical importance; thus n = 1 and n = 2 yield immediately the linear and parabolic functions respectively. With a slight rearrangement of constants the function above can be written in the form:

$$V = \alpha (z + A)^{\frac{1}{n}} \qquad (8a)$$

(II) $$V = V_o (1 + kz) \qquad (9)$$

The velocity is a linear function of depth. This is a special case of (I) with n = 1 and is the one most commonly treated in literature.

(III) $$V = V_o (1 + kz)^{\frac{1}{2}} \qquad (10)$$

The velocity is a parabolic function of depth. This is a special case of (I) with n = 2, and has enjoyed a certain degree of popularity in literature. This function has been used by Rice [16] as a basis for comparing several standard computing techniques and by Stulken [17] in an analysis of the errors in straight-ray computing methods.

(IV) $$V = V_o (1 + kz)^{\frac{1}{3}} \qquad (11)$$

This is a special case of (I) with n = 3.

(V) $$V = V_o + Az^{\frac{1}{n}} \qquad (12)$$

This function bears a superficial resemblance to the binomial expression of case (I). Rutherford (1947) has computed the depth to a high-speed layer for the case where the overburden velocity is of this form with the exponent
n = 2.

(VI) $$V = Az^{\frac{1}{n}} \qquad (13)$$

This special case of (V) with $V_o = 0$ represents an important group of functions having zero initial velocity. Some of the properties have been discussed by Goguel [18]. The functions are finding increasing use in applications to weathering problems.

(VII) $$V = V_o e^{kz} \qquad (14)$$

The velocity increases exponentially with depth (for k > 0). An analysis of this function has been given by Slotnick [3], and an application to the fitting of empirical data discussed by Mott-Smith [19].

(VIII) $$V = V_1 \tanh(Az + B) \quad (15)$$

The velocity increases from $V_o (= V_1 \tanh B)$ following the form of the hyperbolic tangent function to a limiting value of V_1.

(IX) $$V = V_1 - \left[\frac{A}{(z+a)}\right] \quad (16)$$

The function represents a rectangular hyperbola with centre at $V = V_1,\ z = -a$. The velocity increases from $V_o \left(= V_1 - (\frac{A}{a})\right)$ hyperbolically to a limiting value of V_1.

(X) $$V = V_o \left[1 - \left(\frac{z}{z_o}\right)^2\right]^{-1/2} \quad (17)$$

Here the velocity approaches infinity at the finite depth $z = z_o$

(XI) $$V = V_o \left(1 + A^2 z^2\right)^{1/2} \quad (18)$$

This function bears a superficial resemblance to the parabolic function considered in case (III).

(XII) $$V = A\left[\frac{z}{z(z+h)}\right]^{1/2} \quad (19)$$

The velocity increases from zero to a limiting value of A.

Of all these functions, the type with considerable importance is the oldest, simplest, and most widely used linear model [3, 20]). Together with its simplicity, experience shows that the V_o-K technique tends to work well in clastic sections, hence the choice of the linear instantaneous velocity depth-profile as a basis for this study.

3.3 Velocity Modelling

Velocity modelling is a physical or mathematical concept from which seismic velocity variations and effects can be deduced for better understanding of geophysical observations and subsurface geology. Different kinds of velocity models are known to exist and are required for different purposes (For example, stacking, migration, or depth conversion).

3.3.1 Piecewise-Constant Velocity Model

This conventional method of interpretation of seismic data involves fitting Time-Distance curves as linear segments (Fig. 3). This type of model assumes that velocity is constant within each medium, ray paths are straight, and layering is in discrete steps in a sedimentary region and that true increase in velocity continues downward indefinitely. Based on these assumptions, the velocities and depths to different horizons in a media are calculated from intercept time and cross-over distances for various layers. The velocity of each layer here is obtained from the inverse of the slope of the line segments corresponding to that layer in the time-distance graph. The velocity calculated from the inverse slope of each line segment indicates the mean for the discrete velocities of each thin layer in range. This could not be said to be very accurate because of the inability of refraction in this case to resolve small changes in density or acoustic impedance contrast in response to gradual changes in lithology with depth. When there is no abrupt change of lithology and no large scale variation in the thickness of the main rock units as is the case in the Niger Delta, intercept time and cross-over distances become complex or break down completely because the time-distance line graph would be a smooth curve instead of distinct line segments. This is the case with many sedimentary basins of the world.

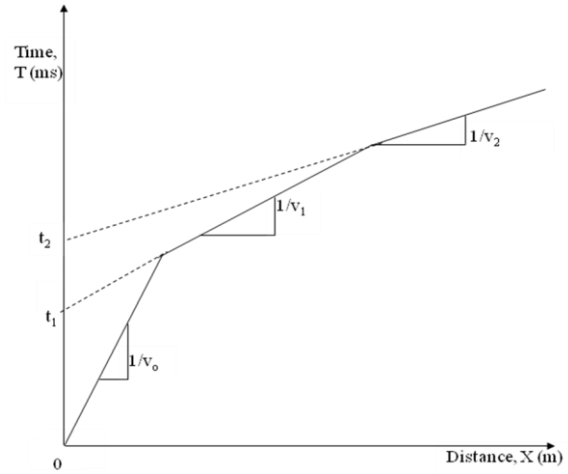

Fig. 3: Time-Distance graph for the discrete layers case models

3.3.2 Linear Increase of Velocity with Depth Models

In many sedimentary basins of the world such as the Niger Delta, the lithology actually tends to change gradually with depth of burial rather than in discrete steps at boundaries as widely assumed before now. Velocity in such basins increases continuously with depth because of differential compaction effects. By reason of its simplicity and close correspondence to the actual Velocity-Depth relationship in most clastic sedimentary materials, the function is given by:

$$V(z) = V_o + kz \tag{20}$$

where $V(z)$ = velocity at depth, z below the surface, V_0 = top-interface instantaneous velocity, k = constant (velocity gradient). This has extensively been employed to represent the velocity variation in sedimentary basins [4]. The dimensions of $V(z)$ and V_o are metres per second and that of z is metres. This implies that the dimension of k is per second or better stated metres per second per metre. The value of k is the increase in velocity per unit depth or the acceleration factor. This value is generally between 0.3 and 1.3 per second [21].

Refracted waves through a section with this kind of lithology can be visualized by assuming a series of thin layers, each of higher velocity than the one above and pass to the limit of an infinite number of infinitesimally thin members (Fig. 4). Such limits correspond to a section having a continuous increase of velocity with depth. The ray path would then have the form of a smooth curve which is convex downward, and then the time-distance curve, also smooth would be convex upward [4].

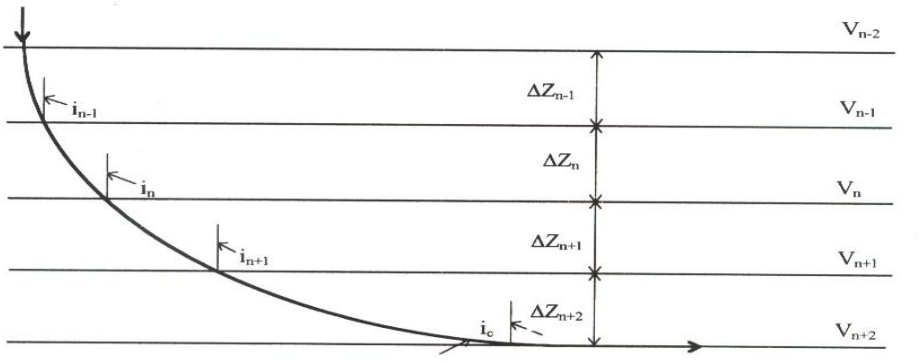

Fig. 4: Ray path on the side toward the shot for series of thin layers with small increments of velocity between them.

Any medium as that described in Figure 4 in which the velocity increases linearly with depth, the wave paths are arcs of circles whose centres lie at a distance V_o/k above the horizontal line on the surface and a radius such that the rays will reach the refractor at a point having X coordinate mid-way between that of the source

and of the receiver (Fig. 5). The refraction time-distance curve for formations of linear increase of velocity with depth is well approximated by a simple hyperbolic function given by Slotnick [20]:

$$T = \frac{2}{k}\sinh^{-1}\frac{kx}{2V_o} \qquad (21)$$

where T = Time of arrival in seconds, k = Velocity gradient in per seconds, x = Distance between shot point and receiver, V_o = Velocity at depth zero (along the first layer).

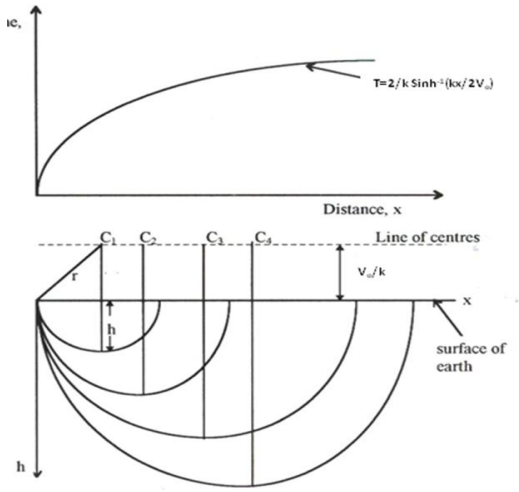

Fig. 5: Ray path and Time-Distance curve for linear increase of velocity with depth.

3.3.2.1 Wave Path Theory

Slotnick [20] had shown that in a medium in which the velocity increases with depth the function $V = V_o + kz$ holds. The wave paths are arcs of circles whose centre lie at a distance V_o/k above the surface. In particular, in a vertical section through a shot point through a line (of geophones) on the surface, the wave paths are circular arcs through the shot point whose centres lie on the line parallel to and at a distance V_o/k above the line on the surface as shown in Fig. 6. Each circle has its centre at the point with the coordinates $C:\left[\left(1-p^2V_o^{\,2}\right)^{1/2}/kp, -V_o/k\right]$ where $1/kp$ is the radius of the circle passing through the shot point at origin, O; p (ray parameter) is the slope of the Time-Distance curve (dT/dX) at any point of emergence of a particular ray on the earth's surface.

3.3.2.2 Wave Front Theory

Consider a hypothetical subsurface consisting of two media, each with uniform clastic sedimentary properties, the upper separated from the lower by a horizontal interface at depth, z (Fig. 7). The velocity of seismic wave in the upper layer is V_0 and that in the lower, V_1 with $V_1 > V_o$. A seismic wave generated at a point O on the surface has energy travelling out from it in hemispherical wave fronts. When the spherical wave fronts from O strikes the interface, where the velocity changes, the energy will be refracted into the lower medium according to Snell's law.

The process is demonstrated in Fig. 7 for the time corresponding to six wave fronts. At point A on wave front 4, the tangent to the sphere in the lower medium becomes perpendicular to the boundary. The ray passing through the point now begins to travel along the boundary with the velocity of the lower medium. Thus, by definition, the ray OA strikes the interface at a critical angle ($Sin^{-1}(V_o/V_1)$). For the case of linear increase of velocity with depth, consider Fig. 8. Here, the mid-point Q of the line OP has the coordinates $(x/2, h/2)$. The slope OP is x/h. Accordingly, the slope QC, the perpendicular bisector of line OP is $-x/h$. The equation of QC is therefore:

$$xX + hH - (x^2 + h^2)/2 = 0 \qquad (22)$$

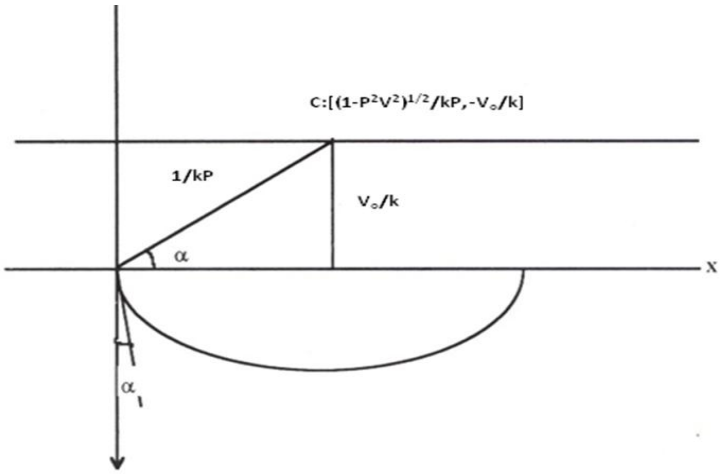

Fig. 6: Circular wave path pertaining to the particular value of the parameter, p.

Hence, the travel time from the shot point O to the point P: (x,h) in this medium is given by the relation:

$$t = (1/k)Cosh^{-1}\left[\left\{1+k^2\left(x^2+h^2\right)\right\}/\left\{2V_o\left(V_o+kh\right)\right\}\right] \qquad (23)$$

The equations of the wave are now immediately apparent. They are defined as been the loci of the point for which the travel time is the same. Accordingly, in Equation (24), the travel time is assigned a specific value T; this locus is obtained by setting $t = T$. By rearranging the terms, we have:

$$2V_o\left[V_o+kh\right]\left[Cosh(aT)-1\right] = a^2\left[x^2+h^2\right] \qquad (24)$$

This implies that:

$$X^2 + \left\{\left[h-\left[V_o/k\right]\left[Cosh\left(kT-1\right)\right]\right]\right\}^2 = \left[V_o^{\,2}/k^2\right]Sinh(xkT) \qquad (25)$$

Interpreting Equation (6) geometrically, the wave fronts are circles whose centres are along the h - axis at the points $\{0,\left[V_o/k\right]\left[Cosh(kT)-1\right]\}$ and whose radii are $\left[V_o/k\right]Sinh(kT)$, where T = the travel time corresponding to each wave front.

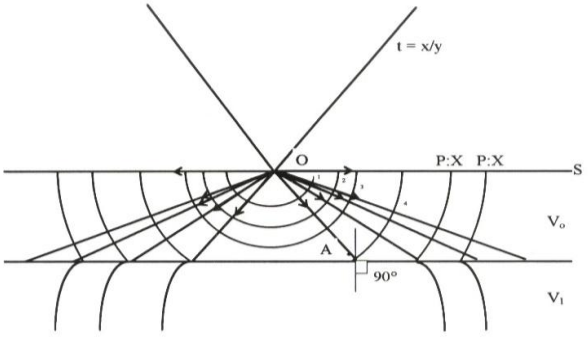

Fig. 7: A hypothetical subsurface consisting of two media each with uniform elastic properties

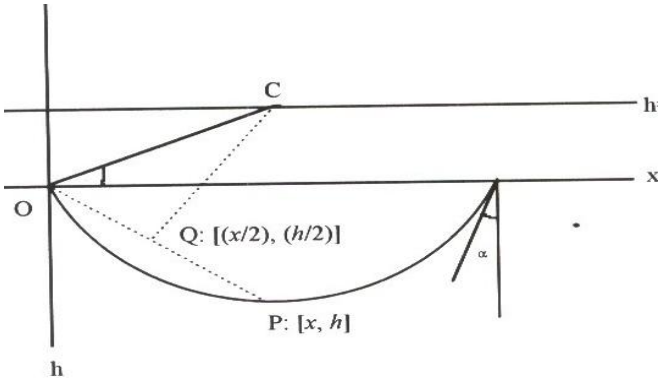

Fig. 8: Typical wavefront for the case of a linear increase of velocity with depth

IV. Materials, Methods and Discussion

4.1 Generation of Model Curves

The linear increase of instantaneous velocity with depth model is illustrated with seismic refraction first breaks data acquired from a 3D reflection survey in the central Niger Delta. The various first breaks and the determined geophone offsets are shown in Table 1. Fig. 9 shows a typical refraction time-distance curve fitted for the model employing a linear increase of instantaneous velocity with depth. It can be noticed that there is an increase in arrival time with distance from the shot to the receiver. This results from the fact that the length of the travel path of the refracted waves becomes greater at larger offset distances from the shot point. To obtain smooth curve, it was constrained that the plot must start from the origin, that is (T, X) = (0, 0) and that all values less than the previous entry in the Table should be ignored.

A visual examination of the sequence of the plotted points in Fig. 9 shows that a "smooth" curve of the anti-hyperbolic sine type fits the data.

Table 1: Typical First-Breaks Data

Trace No.	First Break Times (ms)	Geophone Offset (m)
1	129.60	176.63
2	126.50	176.72
3	140.80	190.23
4	133.60	190.46
5	145.10	215.40
6	167.90	248.34
7	192.50	286.12
8	216.50	327.10
9	239.00	370.45
10	271.30	414.99
11	292.50	460.83
12	324.50	507.55
13	354.20	554.63
14	385.90	602.11
15	416.00	650.21
16	430.80	698.48
17	457.10	747.10
18	484.60	795.58
19	527.50	844.52
20	543.70	893.39
21	567.50	942.47
22	600.00	991.40
23	619.20	1041.10
24	645.80	1090.24
25	714.90	1189.24
26	740.20	1236.59
27	762.90	1237.91
28	783.30	1327.96
29	804.00	1361.62
30	825.80	1394.95

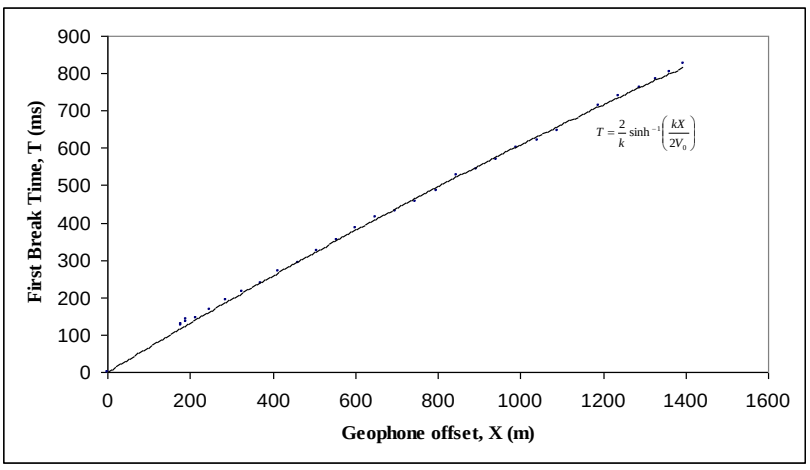

Fig. 9: Refraction Time-Distance Curve for Linear Distribution of Velocity

4.2 Computation of model parameters

The model parameters k and V_0 can now be determined since the data yields to the theory of linear increase of instantaneous velocity with depth. Considering the data in Table 1, the parameters k and V_o are determined analytically using the relationship (Equation 21) of the form:

$$T = \frac{2}{k}\sinh^{-1}\frac{kx}{2V_o}$$

Or equivalently:

$$Sinh(\frac{kT}{2}) = \frac{kx}{2V_o} \qquad (26)$$

Mathematically, k and V_0 are two unknowns to be determined. At least two conditions are therefore required. Now, three sets of data are chosen from Table 1 as follows:

X = 415 m; T = 271.3 ms = 0.2713 s
X = 845 m; T = 527.5 ms = 0.5275 s
X = 1328 m; T = 783.3 ms = 0.7833 s

Substituting into Equation (7) we obtain:

$$Sinh\left(\frac{0.2713\,k}{2}\right) = \frac{415\,k}{2V_o} \qquad (27a)$$

$$Sinh\left(\frac{0.5275\,k}{2}\right) = \frac{845\,k}{2V_o} \qquad (27b)$$

$$Sinh\left(\frac{0.7833\,k}{2}\right) = \frac{1328\,k}{2V_o} \qquad (27c)$$

Dividing 27(b) by 27(a) we have:

$$Sinh(0.5275\,k) = 2.036\,Sin(0.27133\,k) \qquad (28a)$$

Again dividing 27(c) by 27(b) we have:

$$Sinh(0.7833\,k) = 1.5716\,Sin(0.5275\,k) \qquad (28b)$$

Similarly, dividing 27(c) by 27(a), we obtain:

$$Sinh(0.7833\,k) = 3.2Sin(0.2713\,k) \qquad (28c)$$

The solution is sought in Tables 2 (a), (b) and (c) and Figs. 10 (a), (b), and (c) below:

In column I of the Tables, the values of k are given in the range (0.1 to 1.3) in which the solution might be expected to fall. Columns II, III, IV and V are obtained by multiplication as indicated by the headings of those columns, motivated by Equations 28 (a), (b), and (c). Column VI is obtained by the multiplication as indicated. The place where columns III and VI have equal values for the same value of k is sought.

A study of Table 2 indicates that this occurs between k = 1.15 and 1.2. This problem is reduced to a graphic solution as shown in Fig. 10 (a) in which columns III and VI are plotted as functions of k and the intersect found.

Table 2 (a): Analytical Solution for Equation 28 (a)

I	II	III	IV	V	VI
K	.5275K	SINH(.5275K)	.2713K	SINH(.2713K)	2.036SINH(.2713K)
0.1	0.05275	0.0528	0.02713	0.02713	0.0552
0.15	0.07913	0.0792	0.040695	0.04071	0.0829
0.2	0.10550	0.1057	0.05426	0.05429	0.1105
0.25	0.13188	0.1323	0.067825	0.06788	0.1382
0.3	0.15825	0.1589	0.08139	0.08148	0.1659
0.35	0.18463	0.1857	0.094955	0.09510	0.1936
0.4	0.21100	0.2126	0.10852	0.10873	0.2214
0.45	0.23738	0.2396	0.122085	0.12239	0.2492
0.5	0.26375	0.2668	0.13565	0.13607	0.2770
0.55	0.29013	0.2942	0.149215	0.14977	0.3049
0.6	0.31650	0.3218	0.16278	0.16350	0.3329

0.65	0.34288	0.3496	0.176345	0.17726	0.3609
0.7	0.36925	0.3777	0.18991	0.19105	0.3890
0.75	0.39563	0.4060	0.203475	0.20488	0.4171
0.8	0.42200	0.4346	0.21704	0.21875	0.4454
0.85	0.44838	0.4636	0.230605	0.23265	0.4737
0.9	0.47475	0.4928	0.24417	0.24660	0.5021
0.95	0.50113	0.5224	0.257735	0.26060	0.5306
1	0.52750	0.5523	0.2713	0.27464	0.5592
1.05	0.55388	0.5826	0.284865	0.28873	0.5879
1.1	0.58025	0.6134	0.29843	0.30288	0.6167
1.15	0.60663	0.6445	0.311995	0.31708	0.6456
1.2	0.63300	0.6761	0.32556	0.33134	0.6746
1.25	0.65938	0.7082	0.339125	0.34566	0.7038
1.3	0.68575	0.7408	0.35269	0.36005	0.7331

From Fig. 10(a), we have that k = 1.17 s^{-1}. So from Equation (27a):

$$Sinh(0.10865\,k) = \frac{207.5k}{V_o} \tag{29}$$

$$Sinh(0.1271) = \frac{242.78}{V_o} \tag{30}$$

$$0.12744 = \frac{242.78}{V_o}$$

$$\Rightarrow V_o = \frac{242.78}{0.12744} = 1905 ms^{-1}$$

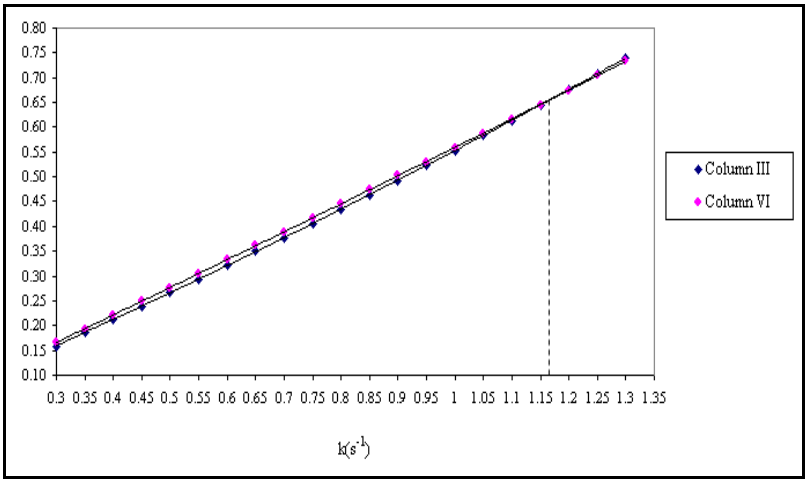

Fig. 10 (a): Graphical solution of Equation 28 (a)

A study of Table 2 (b) indicates that the place where the solution occurs is between k = 1.00 and 1.05. This problem is also reduced to a graphic solution as shown in Fig. 10 (b) in which columns III and VI are plotted as functions of k and the intersect found.

Table 2 (b): Analytical Solution for Equation 28 (b)

I	II	III	IV	V	VI
K	.7833K	SINH(.7833K)	.5275K	SINH(.5275K)	1.5716SINH(.5275K)
0.1	0.07833	0.0784	0.05275	0.05277	0.0829
0.15	0.117495	0.1178	0.079125	0.07921	0.1245
0.2	0.15666	0.1573	0.1055	0.10570	0.1661
0.25	0.195825	0.1971	0.131875	0.13226	0.2079

0.3	0.23499	0.2372	0.15825	0.15891	0.2497
0.35	0.274155	0.2776	0.184625	0.18568	0.2918
0.4	0.31332	0.3185	0.211	0.21257	0.3341
0.45	0.352485	0.3598	0.237375	0.23961	0.3766
0.5	0.39165	0.4017	0.26375	0.26682	0.4193
0.55	0.430815	0.4443	0.290125	0.29421	0.4624
0.6	0.46998	0.4875	0.3165	0.32181	0.5058
0.65	0.509145	0.5314	0.342875	0.34963	0.5495
0.7	0.54831	0.5762	0.36925	0.37770	0.5936
0.75	0.587475	0.6219	0.395625	0.40603	0.6381
0.8	0.62664	0.6685	0.422	0.43464	0.6831
0.85	0.665805	0.7161	0.448375	0.46355	0.7285
0.9	0.70497	0.7648	0.47475	0.49279	0.7745
0.95	0.744135	0.8147	0.501125	0.52236	0.8209
1	0.7833	0.8659	0.5275	0.55231	0.8680
1.05	0.822465	0.9184	0.553875	0.58263	0.9157
1.1	0.86163	0.9723	0.58025	0.61336	0.9640
1.15	0.900795	1.0277	0.606625	0.64452	1.0129
1.2	0.93996	1.0846	0.633	0.67613	1.0626
1.25	0.979125	1.1432	0.659375	0.70820	1.1130
1.3	1.01829	1.2036	0.68575	0.74077	1.1642

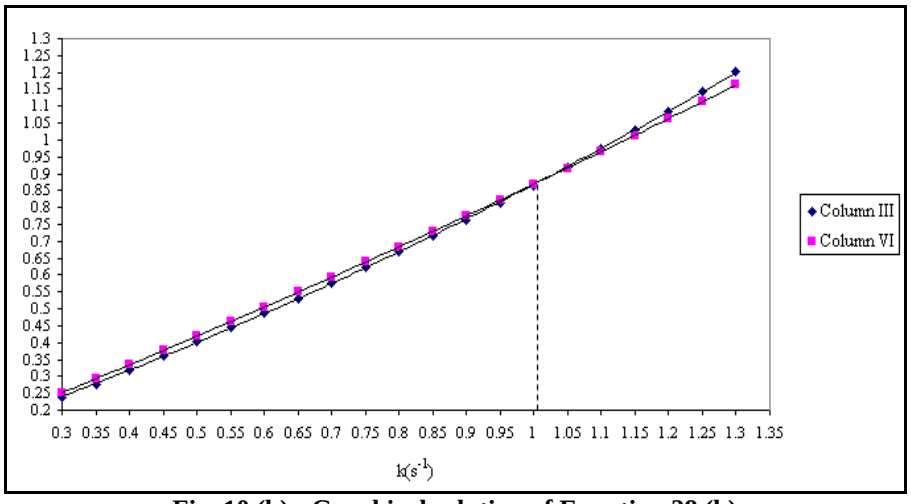

Fig. 10 (b): Graphical solution of Equation 28 (b)

From Fig. 10 (b), we have that k = 1.01 s^{-1}. So from Equation (27c):

$$Sinh(0.39165\,k) = \frac{664\,k}{V_o} \tag{31}$$

$$Sinh(0.39557\,) = \frac{670.64}{V_o} \tag{32}$$

$$0.40597\ = \frac{670.64}{V_o}$$

$$\Rightarrow V_o = \frac{670.64}{0.40597} = 1652 ms^{-1}$$

A study of Table 2 (c) indicates that the place where the solution occurs is between k = 1.05 and 1.10. This problem is similarly reduced to a graphic solution as shown in Fig. 10 (c) in which columns III and VI are plotted as functions of k and the intersect found.

Table 2 (c): Analytical Solution for Equation 28 (c)

I	II	III	IV	V	VI
K	.7833K	SINH(.7833K)	.2713K	SINH(.2713K)	3.2SINH(.2713K)
0.1	0.07833	0.07841	0.02713	0.02713	0.08683
0.15	0.117495	0.11777	0.040695	0.04071	0.13026
0.2	0.15666	0.15730	0.05426	0.05429	0.17372
0.25	0.195825	0.19708	0.067825	0.06788	0.21721
0.3	0.23499	0.23716	0.08139	0.08148	0.26074
0.35	0.274155	0.27760	0.094955	0.09510	0.30431
0.4	0.31332	0.31847	0.10852	0.10873	0.34795
0.45	0.352485	0.35983	0.122085	0.12239	0.39164
0.5	0.39165	0.40174	0.13565	0.13607	0.43541
0.55	0.430815	0.44427	0.149215	0.14977	0.47926
0.6	0.46998	0.48747	0.16278	0.16350	0.52320
0.65	0.509145	0.53143	0.176345	0.17726	0.56723
0.7	0.54831	0.57620	0.18991	0.19105	0.61137
0.75	0.587475	0.62186	0.203475	0.20488	0.65562
0.8	0.62664	0.66846	0.21704	0.21875	0.69999
0.85	0.665805	0.71610	0.230605	0.23265	0.74449
0.9	0.70497	0.76483	0.24417	0.24660	0.78913
0.95	0.744135	0.81474	0.257735	0.26060	0.83391
1	0.7833	0.86589	0.2713	0.27464	0.87885
1.05	0.822465	0.91838	0.284865	0.28873	0.92395
1.1	0.86163	0.97227	0.29843	0.30288	0.96921
1.15	0.900795	1.02766	0.311995	0.31708	1.01466
1.2	0.93996	1.08462	0.32556	0.33134	1.06029
1.25	0.979125	1.14324	0.339125	0.34566	1.10612
1.3	1.01829	1.20362	0.35269	0.36005	1.15215

From Fig. 10 (c), we have that k = 1.07 s^{-1}. So from Equation (27b):

$$Sinh(0.26375\,k) = \frac{422.5k}{V_0} \tag{33}$$

$$Sinh(0.28221) = \frac{452.075}{V_0} \tag{34}$$

$$0.28597 = \frac{452.075}{V_0}$$

$$\Rightarrow V_0 = \frac{452.075}{0.28597} = 1581 ms^{-1}$$

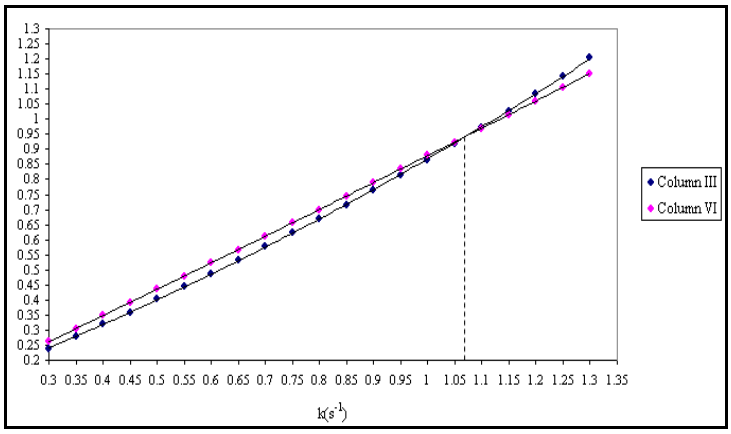

Fig. 10 (c): Graphical solution of Equation 28 (c)

4.3 Velocity Gradient Function

The computed model parameters by the graphical method are shown in the Table 3 below.

Table 3: Computed model parameters

S/No.	K (s^{-1})	V_0 (m/s)
1	1.17	1905
2	1.01	1852
3	1.07	1581
Average	1.083	1712.7

These imply that the velocity gradient function by Equation (20) is:

$$V = 1712.7 + 1.083z \qquad (35)$$

or

$$V = 1.7127 + 1.083z\,;$$

where V_0 is now in kms^{-1}.

4.4 Construction of Raypaths

As stated earlier that in a medium in which the velocity increases linearly with depth, that is, $V = V_0 + kz$, the wave paths emanating from a shot point O at the surface are arcs of circles passing through O whose centres lie at a distance V_0 / k above the surface. The coordinate of the centre is given as:

$$C : \left[\left(1 - p^2 V_0^{\,2}\right)^{1/2} / kp, -V_0 / k\right]$$

where p = slope of the time-distance curve at any point of emergence of the wave path (at geophone location). Its radius is $1/kp$ and it passes through the shot-point O. This principle is used to construct all the ray paths for the shots in the survey. For the typical field data shown in Table 1, the centre and radius of each raypath is computed in Table 4 and plotted in Fig. 11. But before this is done, the ray parameter, p and the emergence angle, α_0 would first of all be determined.

Suppose we choose any point P, say 844.52 m from O as a typical point. The travel time from O to P is 0.5275 s as shown in Table 1. The emergence angle, α_0 at P is obtained from the equation:

$$X_P = \left(\frac{2V_o}{k}\right) Cot\alpha_o = P \qquad (36)$$

This implies that: $844.52 = 2\left(\frac{1712.67}{1.08}\right) Cot\alpha_o \Rightarrow Cot\alpha_o = 0.267014\ ,\ \alpha_o = 75°$

We also have that: $Sin\alpha_o / V_o = p\,,$ (37)

So we have: $p = 0.96593 / 1712.67 = 5.6398829 \times 10^{-4}\, sm^{-1}$

This typical value of p is the one that singles out the wave path to P from all wave paths. It is also the value of the slope dt/dx of the time-distance curve at P. This process is repeated for all the time-distance data in Table 1.

Table 5: Parameters for the Construction of Raypaths

X (m)	$p=Sin\alpha_o/V_o$ X 10^{-4}(s/m)	$p^2V_o^2$ X 10^{-1}	$[1- p^2V_o^2]^{1/2}/kp$ (m)	1/kp (m)
176.63	5.8298	9.9689	88.3	1583.9
176.72	5.8297	9.9686	88.4	1583.9
190.23	5.8283	9.9639	95.1	1584.3
190.46	5.8282	9.9638	95.2	1584.3
215.4	5.8253	9.9538	107.7	1585.1
248.34	5.8209	9.9387	124.2	1586.3
286.12	5.8151	9.9188	143.1	1588.0
327.1	5.8079	9.8944	163.4	1590.0
370.45	5.7992	9.98647	182.2	1592.2
414.99	5.7893	9.9831	207.4	1595.0
460.83	5.7778	9.7921	230.4	1598.1
507.55	5.7650	9.7488	254.0	1606.7
554.63	5.7519	9.7044	276.0	1605.3
602.11	5.7358	9.6502	301.0	1609.8
650.21	5.7226	9.6059	320.3	1613.5
698.48	5.7015	9.5352	349.2	1619.5
747.1	5.6825	9.4716	373.5	1625.0
795.58	5.6624	9.4049	397.8	1630.7
844.52	5.6425	9.3388	420.8	1636.4
893.39	5.6191	9.2614	446.6	1643.3
942.47	5.5958	9.1848	471.1	1650.1
991.40	5.5717	9.1057	495.6	1657.3
1041.10	5.5467	9.0245	520.0	1664.7
1090.24	5.5201	8.9379	545.2	1672.7
1189.24	5.4655	8.7621	594.4	1689.4
1236.59	5.4381	8.6746	618.2	1698.0
1237.91	5.4374	8.6722	618.8	1698.2
1327.96	5.3834	8.5008	664.1	1715.2
1361.62	5.3636	8.4367	680.7	1721.7
1394.95	5.3423	8.3715	697.5	1728.4

4.5 Construction of Wavefronts

As discussed earlier on that at any given time, T, the wavefront has Radius = $(V_o/k)SinhkT$ and Centre: $\{0, (V_o/k)[Cosh(kT-1)]\}$. The values of k and V_0 have been substituted for and the dimensions of the radii and centres of the wave fronts computed in Table 5. The wave fronts for the various values of T, the travel-time corresponding to each wave front, in Table 1 are constructed as shown in Fig. 11. It can be noticed that the wave paths and wave fronts in Fig. 11 cut each other at right angles. This implies that through every point in a vertical section in our medium, the wave path circles and the wave front circles cut at 90^o.

4.5.1 Computation of Maximum of Penetration, z_{max}

Here the depth which is indicated by z_{max} is given as:

$$Sin\alpha = Sin90° = 1 = p\left(V_o + kz_{\max}\right)$$

$$\Rightarrow z_{\max} = \frac{\left(1 - pV_o\right)}{kp} \qquad (38)$$

Equation (38) is used to compute the maximum depth of penetration for all the rays emerging at the various offsets on the surface from the shotpoint. The results are shown in Table 6. The velocities at these various depths for the wave paths are also computed in Table 6 using the velocity gradient Equation given as:

$$V = 1712.7 + 1.083z$$

Table 5: Parameters for the Construction of Wavefronts

T (s)	kT	R = (V_0/k)SinhkT	(V_0/k)Cosh(kT -1)
0.1296	0.1404	222.8	15.6
0.1265	0.1370	217.3	14.9
0.1408	0.1525	242.1	18.4
0.1336	0.1447	229.6	16.6
0.1451	0.1571	249.5	19.6
0.1679	0.1818	289.1	26.2
0.1925	0.2085	332.1	34.5
0.2165	0.2345	374.3	43.7
0.2390	0.2588	414.0	53.3
0.2713	0.2938	471.3	68.8
0.2925	0.3168	509.4	80.0
0.3245	0.3514	567.2	98.7
0.3542	0.3836	621.6	117.8
0.3859	0.4179	678.7	140.1
0.4160	0.4505	736.8	163.2
0.4308	0.4666	765.0	175.3
0.4571	0.4951	815.3	197.8
0.4846	0.5248	868.6	222.8
0.5275	0.5713	953.4	265.2
0.5437	0.5888	986.0	282.1
0.5675	0.6146	1034.3	308.2
0.6000	0.6498	1101.5	345.8
0.6192	0.6706	1141.8	369.1
0.6458	0.6994	1198.4	402.8
0.7149	0.7742	1350.4	498.1
0.7402	0.8016	1408.0	536.0
0.7629	0.8262	1460.4	571.2
0.7833	0.8483	1508.3	604.0
0.8040	0.8707	1557.6	638.3
0.8258	0.8943	1610.5	675.7

4.5.2 The Velocity Model

A plot of V_{max} against z_{max} data in Table 6 for each of the wave paths shown in Fig. 11 gives us a velocity model trend shown in Fig. 12. The trend shows a linear model which implies that velocity increases linearly with depth in this region of the Niger Delta.

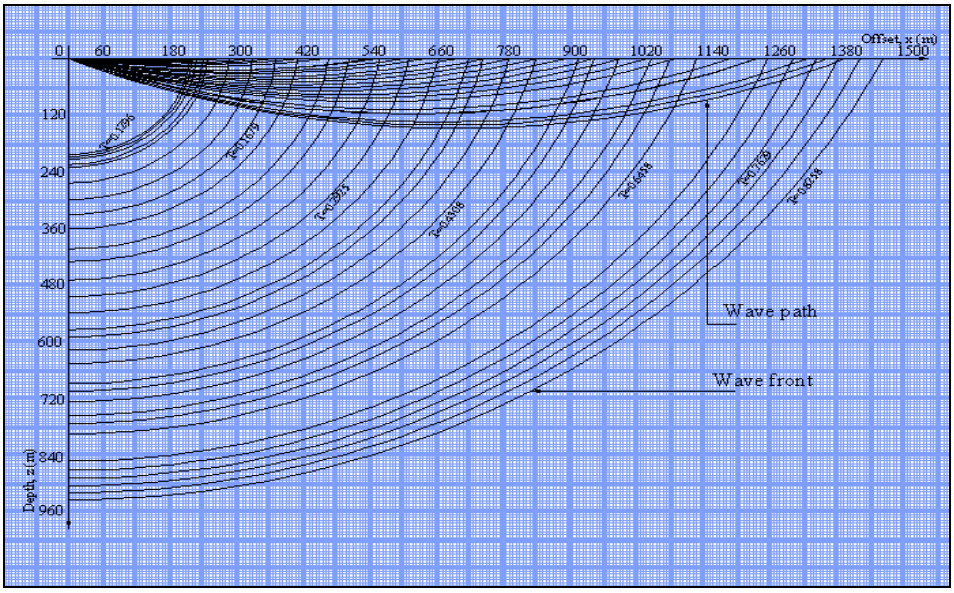

Fig. 11: Typical construction of wave paths and wavefronts for the field data example

Table 6: Computed Maximum Depth of Penetration, z_{max} and corresponding V_{max}

X (m)	z_{max} (m)	V_{max} (m/s)
176.63	2.45	1715.32
176.72	2.49	1715.37
190.23	2.87	1715.78
190.46	2.89	1715.80
215.40	3.69	1716.67
248.34	4.89	1717.97
286.12	6.47	1719.68
327.10	8.45	1721.82
370.45	10.84	1724.41
414.99	13.57	1727.37
460.83	16.75	1730.81
507.55	20.31	1734.67
554.63	23.97	1738.63
602.11	28.49	1743.53
650.21	32.21	1747.55
698.48	38.20	1754.04
747.10	43.63	1759.92
795.58	49.41	1766.18
844.52	55.18	1772.43
893.39	62.00	1779.82
942.47	68.88	1787.27
991.40	76.03	1795.01
1041.10	83.52	1803.12
1090.24	91.57	1811.84
1189.24	108.32	1829.98
1236.59	116.86	1839.23
1237.91	117.08	1839.47
1327.96	134.16	1857.97
1361.62	140.51	1864.84
1394.95	147.39	1872.29

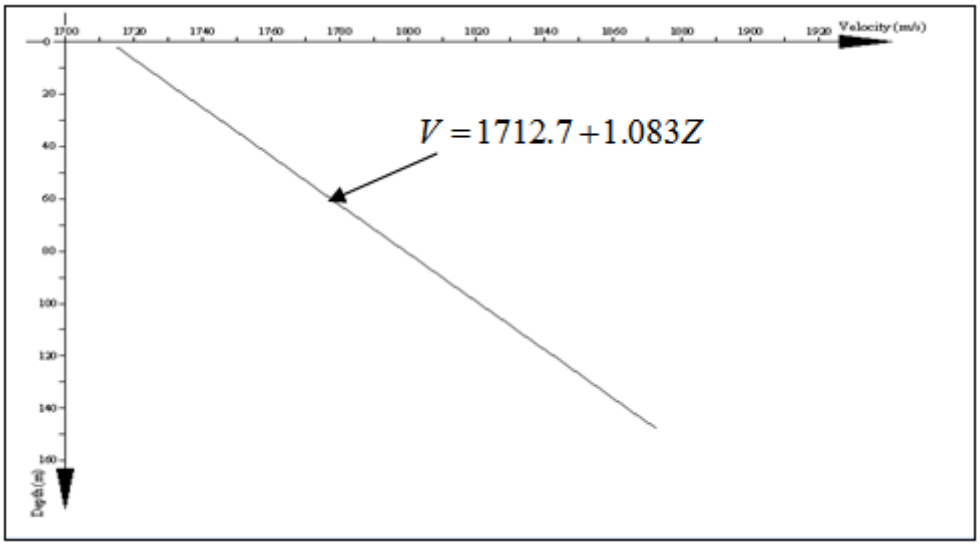

Fig. 12: Typical linear velocity model for the subsurface clastic sediments of the Agbada Region of the Niger Delta.

V. Conclusion

In the Niger Delta sedimentary basin with clastic materials, the time-distance data obtained were observed to yield to the theory of linear increase of velocity with depth, hence the curves generated were hyperbolic in shape. This formed the basis of computation of the model parameters: V_o (top-interface velocity) and k (vertical velocity gradient) by solving the hyperbolic sine equation [Sinh (kt/2) = ($kx/2V_o$) analytically. Computations from a field data example in the central Niger Delta yielded equivalent values of k and V_o as 1.083 s^{-1} and 1,712.7 m/s respectively. The velocity function is represented as: V = 1712.7 + 1.083z. Constructions of raypaths originating from the shot point and emerging at each geophone position were observed to be arcs of circles as obtainable in a case of linear increase of velocity with depth. Similarly constructed wavefronts at the various values of arrival time, T with the equivalent values of k and V_o were observed to be curves which crossed the raypaths at right angles. These results are consistent with theory and go further to show that the developed model obeys all the laws of refraction.

This velocity model can provide a basis for better approximation of the subsurface-clastic sediments structure of the Niger Delta using a relatively small layer thickness. In this case, the assumptions that lithologies are sharply discontinuous and discrete are not considered and this will bring into play the recognition of change in facies, fractures, faults, unconformities and so on and this true in actual field situations.

Acknowledgement

The authors are grateful to Shell Petroleum Development Company (SPDC) of Nigeria for the data used in this work.

References

[1]. Dix, C. H. (1955). Seismic velocity from surface measurements: *Geophysics*, 20, 68-86.
[2]. Hubral, P. and T. Krey, (1980). Interval velocities from seismic reflection time measurement: SEG.
[3]. Slotnick, M.M. (1936). On Seismic Computation with Application I. *Geophysics*, 1 (1), 9-22; Geophysics, 1 (3), 299 - 302.
[4]. Dobrin, M. B. (1983). Introduction to Geophysical Prospecting, Mc Graw-Hill Book Co., London.
[5]. Uko, E. D., Ekine, A. S., Ebeniro, J. O. and Ofoegbu, C. O. (1992). Weathering structure of east central Niger Delta, Nigeria. *Geophysics*, 57 (9), 1228 - 1233.
[6]. Doust H. and Omatsola E. (1990). The Niger Delta: Hydrocarbon Potential of a Major Tertiary Delta Province, Proceedings KNGMG Symposium Coastal Low Lands. *Geology and Geochemistry*, 201 - 237.
[7]. Short, K. C., and Stauble, A. J. (1967). Outline of geology of Niger Delta. *American Association of Petroleum Geologists Bulletin*, 51, 761-799.
[8]. Avbovbo, A. A. (1978). Tertiary Lithostratigraphy of Niger Delta. *American Association of Petroleum Geologists Bulletin*, 62, 295 - 306.
[9]. Whiteman, A. (1982). Nigeria – Its Petroleum Geology Resources and Potential: London, Graham and Trotman p. 394.
[10]. [10]. Faust, L. Y. (1951). Seismic velocity as a function of depth and geologic times. *Geophysics*, 16, 192 - 206.
[11]. Faust, L. Y. (1953). A velocity function including lithologic variation. *Geophysics*, 18, 271 - 288.
[12]. Houston, C. E., (1939). Seismic paths, assuming a parabolic increase of velocity with depth: Geophysics, 4, 242 - 246.
[13]. Al-Chalabi, M. (1997b). Parameter non-uniqueness in velocity versus depth functions. *Geophysics*, 62, 970 - 979.
[14]. Al-Chalabi, M. (1997a). Instantaneous slowness versus depth functions. *Geophysics*, 62, 270 - 273.
[15]. Kaufman, H. (1953). Velocity functions in seismic prospecting *Geophysics*, 18, 289 - 297.
[16]. Rice, R. B. (1950). A Discussion of Steep-Dip Seismic Computing Methods, *Geophysics* XV, 1, 80 - 93.
[17]. [17]. Stulken, E. J. (1945). Effects of Ray Curvature upon Seismic Interpretations, *Geophysics*, X, 4, 472 - 486.
[18]. Goguel, J.M. (1951). Seismic Refraction with variable velocity. *Geophysics*, 16 (1), 81 - 101
[19]. Moth-Smith, M., (1939). On Seismic Paths and Velocity-Time Relations. *Geophysics*, 4 (1), 8 - 23.
[20]. Slotnick, M. M. (1959). Lessons in Seismic Computing, Society of Exploration Geophysicist (SEG), Tulsa, Oklahoma.
[21]. Telford, W. M., L. P. Geldart, P. E. Sheriff, and D. A. Keys (1976). Applied Geophysics. Cambridge University Press, London.

IOSR Journal of Applied Geology and Geophysics (IOSR-JAGG) is UGC approved Journal with Sl. No. 5021, Journal no. 49115.

E. D. Uko, " Seismic Velocity Model for Sedimentary Niger Delta, Nigeria" IOSR Journal of Applied Geology and Geophysics (IOSR-JAGG) 6.5 (2018): 01-18.